Pixel diamond detectors for excimer laser beam diagnostics

M. Girolami*, P. Allegrini, G. Conte, S. Salvatori
S[2]DEL, Solid State and Diamond Electronics Lab, Università degli Studi Roma Tre,
Via della Vasca Navale 84 – 00146, Rome, Italy

ABSTRACT

Laser beam profiling technology in the UV spectrum of light is evolving with the increase of excimer lasers and lamps applications, that span from lithography for VLSI circuits to eye surgery. The development of a beam-profiler, able to capture the excimer laser single pulse and process the acquired pixel current signals in the time period between each pulse, is mandatory for such applications. 1D and 2D array detectors have been realized on polycrystalline CVD diamond specimens. The fast diamond photoresponse, in the ns time regime, suggests the suitability of such devices for fine tuning feedback of high-power pulsed-laser cavities, whereas solar-blindness guarantees high performance in UV beam diagnostics, also under high intensity background illumination. Offering unique properties in terms of thermal conductivity and visible-light transparency, diamond represents one of the most suitable candidate for the detection of high-power UV laser emission. The relatively high resistivity of diamond in the dark has allowed the fabrication of photoconductive vertical pixel-detectors. A semitransparent light-receiving back-side contact has been used for detector biasing. Each pixel signal has been conditioned by a multi-channel read-out electronics made up of a high-sensitive integrator and a Σ-Δ A/D converter. The 500 μs conversion time has allowed a data acquisition rate up to 2 kSPS (Sample Per Second).

Keywords: Excimer lasers, UV detectors, CVD diamond, Beam profiling.

1. INTRODUCTION

Compact and performing UV-beam profilers are getting more and more important, due to an increasing exploitation, in the past few years, of UV sources such as excimer lasers and lamps in a wide range of industrial and research applications, that span from lithography for semiconductor manufacturing in VLSI and MEMS technologies[1] to laser-cutting, from eye surgery[2] to dermatological treatment. State-of-the-art commercially available UV-beam profilers are mainly based on silicon detectors: the deep knowledge of this material in terms of electronic, physical and optical properties, and the well-established technology have encouraged the development and the commercial success of silicon-based UV devices, despite its intrinsic limitations. First, UV-enhanced silicon detectors, though showing a good VUV (vacuum UV) response, still hold a wide spectral responsivity in the visible and near-IR regions[3], with quantum efficiencies that easily reach 80%, and this could be a limiting factor, especially when the detected UV radiation is superimposed to a strong VIS and far-IR background (i.e. solar-blind applications): this problem is generally solved by the interposition of blocking filters between source and detector. The second limitation of silicon devices is important in the analysis of pulsed UV high-power sources (i.e. excimer lasers), that produce fast pulses in the ns time regime: due to the high absorption coefficient of silicon at excimer lasers wavelengths (λ = 193 nm for ArF lasers, λ = 248 nm for KrF lasers), the maximum density of energy that can be transferred to the detector without radiation damage is quite low, and the beam profiler lifetime, for example under 248 nm KrF laser excitation, is limited to 10^5 exposures[4]. These are serious problems, especially for industrial applications that require reliable and long-lasting detectors. To avoid radiation damage, silicon detectors are forced to use attenuators and/or wavelength converters (i.e. fluorescent crystals), so introducing loss factors in terms of spatial resolution, especially for little spot-size laser-beams. In conclusion, excimer laser-beam attenuation is a critical issue for silicon profilers, only settled by striking a balance between performance and costs.

Considering the limitations of silicon in UV detection, a comparative research on alternative semiconductors is desirable. Diamond, member of the wide bandgap semiconductors family, probably represents the best choice for the development of performing, fast and radiation-hard UV detectors[5-8]: the wide bandgap (5.47 eV at 300K) makes it transparent to VIS-

*m.girolami@uniroma3.it; phone 39 06 5733 7201; fax 39 06 5733 7101; http://s2del.uniroma3.it

IR radiations[9-10], reducing dark current (down to few pA) with no need for antireflection coatings or wavelength converters; the high mobility (up to 2000 $cm^2/V \cdot s$) and saturation velocity (~10^7 cm/s) of charge carriers[11] ensure a fast photoresponse (few ns), enabling a real-time monitoring of excimer laser single pulses; finally, the high cohesive energy (7.45 eV/atom) and the highest thermal conductivity (~2000 W/mK) allow to strongly reduce radiation damage, making the employment of attenuators not necessary in case of high-power sources analysis.
This work reports on the realization and test of a compact excimer laser beam profiling system, based on a polycrystalline diamond detector. Multi –strip and –pixel structures have been used for 1D and 2D photodetectors, respectively. A dedicated read-out electronic circuitry has been designed and used to independently sample the signal produced by each strip (or pixel), providing data faster than the repetition rate of the laser pulses: this has enabled a real-time laser beam profile reconstruction.

2. DEVICE REALIZATION AND CHARACTERIZATION

Starting from silicon substrates, thick polycrystalline diamond films have been deposited by MWCVD (Microwave Chemical Vapour Deposition), using a mixture of methane and hydrogen. Silicon has been then removed by a wet etching process, and both nucleation and growth surfaces have been polished through a chemical-mechanical process, removing about 100 µm of material: aim of this treatment is the reduction of growth surface roughness (down to 2 ÷ 8 nm) and the removal of most part of the nucleation material. Only the core section, formed by a well-defined columnar structure, has been selected for the present study, leading to 10 × 10 mm^2, 270 µm thick specimens, with grains average lateral dimension of 200 µm. Selected specimens have been cleaned by an ultrasound treatment for microparticulate removal, followed by a dipping in hot sulphochromic solution for non-diamond phases removal, and a rinse in RCA solution (H_2O_2 + NH_4OH) for chrome residuals removal.
Sandwich contacts have been realized by silver thermal evaporation on the top and bottom faces of the diamond films. The thickness of the bottom electrode, used for device biasing, is only 50 nm, in order to ensure semi-transparence to the impinging UV light, whereas the top contact structure is 200 nm thick. Standard photolithography has been performed to define the array structures shown in fig. 1: the 1D detector consists of a multistrip structure with 32 fingers, 6 mm in length, 80 µm wide and 80 µm apart; the 2D detector is a 36-pixel array (750 × 750 μm^2 each, 150 µm apart).

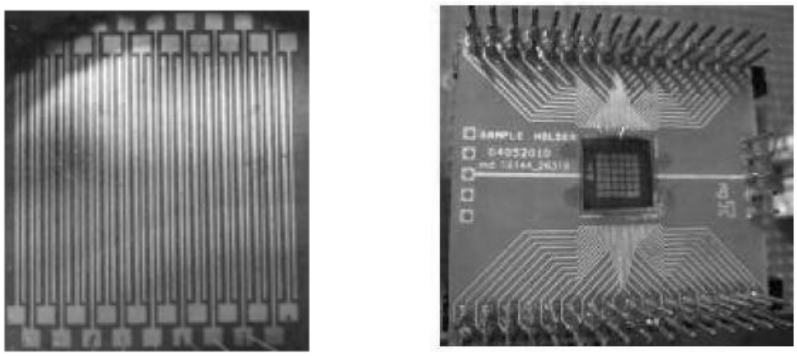

Figure 1. 1D strip detector (left) and 2D pixel detector mounted on a sample holder (right)

Figure 2 shows the operating principle of the realized beam profilers, regardless of the detector type (1D or 2D) and of the electrodes geometry. A semi-transparent top electrode receives impinging photons, whose energy is absorbed by the detector bulk, and converted to electron-hole pairs: a transverse electric field, obtained through a 10 ÷ 40 V bias voltage, allows the separation of photogenerated carriers and their drift towards the electrodes. Each pixel current signal is conditioned by a dedicated front-end electronics, made up of a high-precision switched capacitor integrator and a high-resolution Σ-Δ analog-to-digital converter. The beam-profiling system is then equipped with a microcontroller-based computer-interfaced main board for data acquisition and transfer.

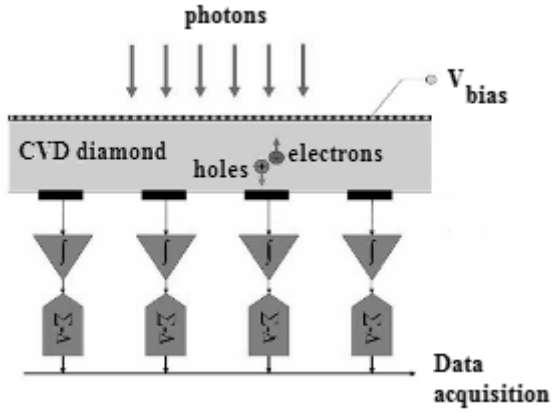

Figure 2. Beam profiler operating principle

An exhaustive study has been conducted in order to preliminarily characterize detectors behavior. Figure 3(a) reports current-voltage characteristics in dark conditions and under UV irradiation (1 μW @ λ = 235 nm): in both cases, contacts ohmicity is ensured up to 100 V bias; dark current is always in the pA range, whereas photocurrent is about 3 orders of magnitude higher. Selected specimens spectral photoconductivity, in terms of normalized quantum efficiency vs. impinging photon energy, is reported in figure 3(b): it's noticeable the high UV-VIS discrimination (about 4 orders of magnitude, comparable to that of a IIa-type natural diamond), a result that confirms diamond detectors suitability for solar blind applications, with no need for filtering or shielding procedures. The most interesting aspect of the selected specimens photoresponse is the over-gap behavior: the very low surface roughness, obtained though polishing, allows to strongly reduce surface recombination, responsible for the over-gap response decrease in non-polished natural diamonds.

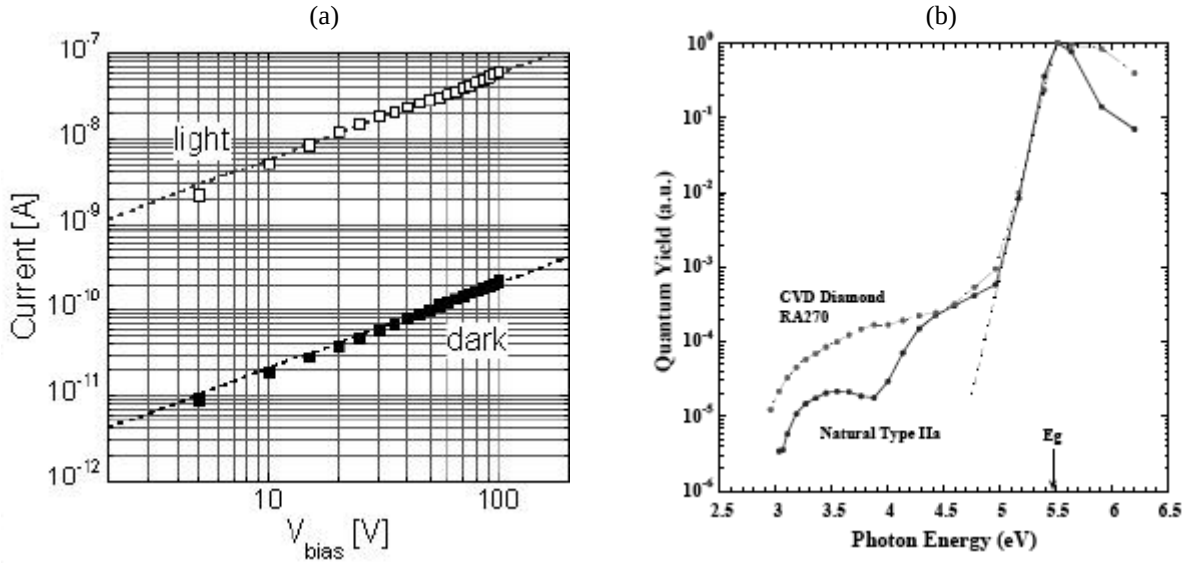

Figure 3. Current-voltage characteristics (a) and spectral photoresponse (b) of the selected diamond specimens

2.1 Dynamic characteristics under excimer laser irradiation

Photoresponse measurements under excimer laser (ArF, λ= 193 nm) irradiation have been performed, aimed to evaluate the detectors response speed and linearity over a wide range of impinging intensities. Temporal evolution of single laser pulses has been preliminarily measured by a vacuum phototube (Hamamatsu H8496-11); then the same measurements have been performed using the realized diamond detectors (V_{bias} =30 V). In both cases, photocurrent has been measured

evaluating the voltage drop on a digital oscilloscope 50 Ω input resistance. Figure 4(a) shows a comparison between vacuum phototube and diamond detector in terms of photoresponse speed: photocurrent pulse rise time (10% to 90% of the peak value) is the same for both devices (~ 1.3 ns), showing the feasibility of a fast, real-time CVD-diamond sensor for excimer laser beam diagnostics.

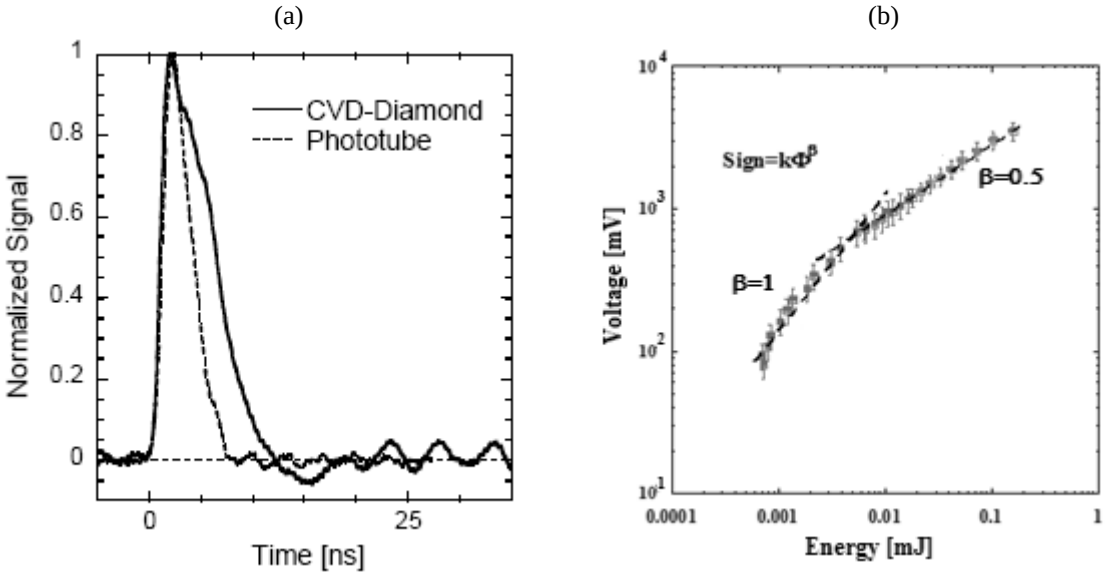

Figure 4. Temporal evolution of excimer laser pulse (a) and photovoltage linearity with impinging energy (b)

In figure 4(b) single-pixel photovoltage peak values are reported as a function of the laser impinging energy. A fairly linear behavior can be observed up to incoming energies of about $5 \cdot 10^{-3}$ mJ, whereas for higher energy laser pulses a transition to a sub-linear photoresponse regime is apparent: consistent with Rose's photoconductivity theory, this transition highlights a shift from a purely monomolecular recombination mechanism (defects-assisted recombination) to a bimolecular one (band-to-band recombination). This result suggests that a certain controlled amount of lattice defects, introduced during CVD diamond growth, can lead to a better UV photoresponse in terms of linearity with impinging laser energy.

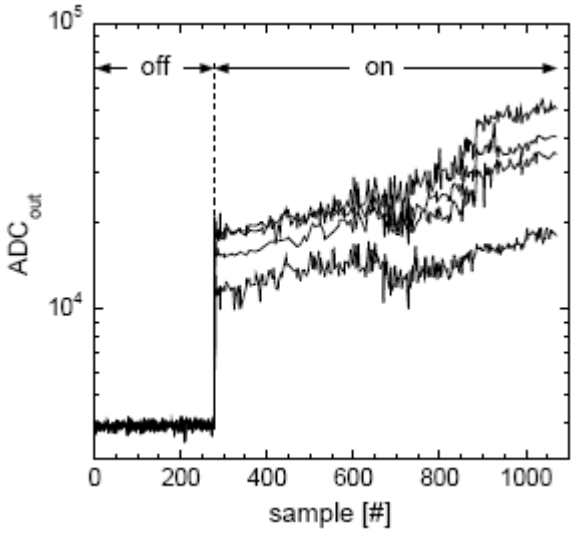

Figure 5. Current signals collected by the 2D detector four central pixels under ArF excimer laser irradiation

After the single-pixel characterization reported above, multi-pixel preliminary measurements have been performed by focusing the laser spot on the 2D detector four central pixels. Figure 5 shows the temporal evolution of the four collected current signals: due to non-uniform spatial distribution of the impinging light, signals are slightly different. The intensity change the laser shows after switching-on is apparent, as well as the increase with time before reaching a steady-state condition (not shown). The response noisy behavior after switching-on is mainly due to two factors: the laser intensity is different at each pulse, especially at higher repetition rates, when laser efficiency strongly decreases; moreover, a noise contribution due to electromagnetic interference (EMI) introduced by the thyratron high frequency generator inside the laser cavity cannot be excluded.

3. BEAM PROFILE MEASUREMENTS

UV beam profiling experiments have been performed in two different ways, as reported in the following sections: first, a low-intensity continuous wave UV spotlight has been used, in order to evaluate 1D and 2D detectors ability to give information on the profile of UV incoherent light sources. Then, 36-pixel 2D detector has been tested for high-power pulsed excimer laser beam monitoring.

3.1 UV lamp beam profiling

Monochromatic UV light source (λ = 235 nm, 5 × 5 mm^2 spot-size) has been selected at the output of a double spectrometer (Spex mod. 1860) coupled to a 300 W arc-discharge Xe-Hg lamp (Perkin Elmer mod. PE 300 BUV). The impinging photon intensity, about 1 μW at the selected 235 nm wavelength, has allowed an easy discrimination of the photocurrent signals, in comparison to the "background" values induced by the diamond sample dark conductivity and the input channels offset errors. A 500 μm wide pinhole, used to irradiate a small portion of the detector area, has been employed for the input channels calibration procedure. The 1D sensor has been then mounted on a micrometric *X*-*Y* moving stage with 10 μm resolution. The calibration procedure has started with the alignment of the spot centroid over the first strip line: successive translations of the array along the vertical direction *Y*, by steps equal to the distance between strips, have allowed the normalization factors evaluation, to take into account during the ordinary "parallel" acquisition of strip-signals. Figure 6 shows the acquired beam profile along the vertical direction *Y*, as result of 100 samples mean values for each strip-signal (total acquisition time 50 ms): it's worth noting the relative low standard deviation values (error bars) of the ADC output codes gained (also ensured by copper-clad shielding of the front-end electronics board).

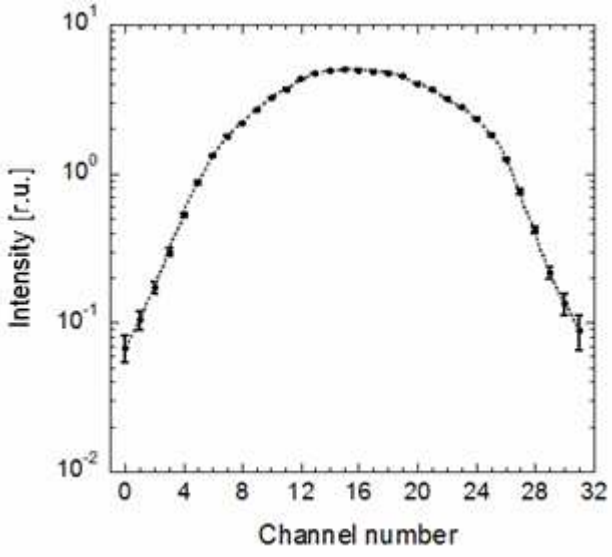

Figure 6. UV Xe-Hg lamp beam one-dimensional profile

Similar results have been obtained for the 36-pixel 2D detector: considering the 32 channels read-out electronics, the four corner pixels have been left disconnected. Using the same 500 μm wide pinhole as 1D case, a similar calibration procedure has been followed: obviously, the micrometric moving stage has been used in this case to move the detector along both *X* e *Y* directions. After calibration, UV spotlight has been positioned on the center of sensor detecting area: starting from this position and keeping *Y* coordinate constant, successive 250 μm-step translations along X axis have been made, acquiring the beam profile at each step, and performing a real-time spot centroid evaluation. Figure 7 reports some of the beam profiles obtained for the 2D detector: the spot centroid shift along X axis through the different detector displacements is apparent.

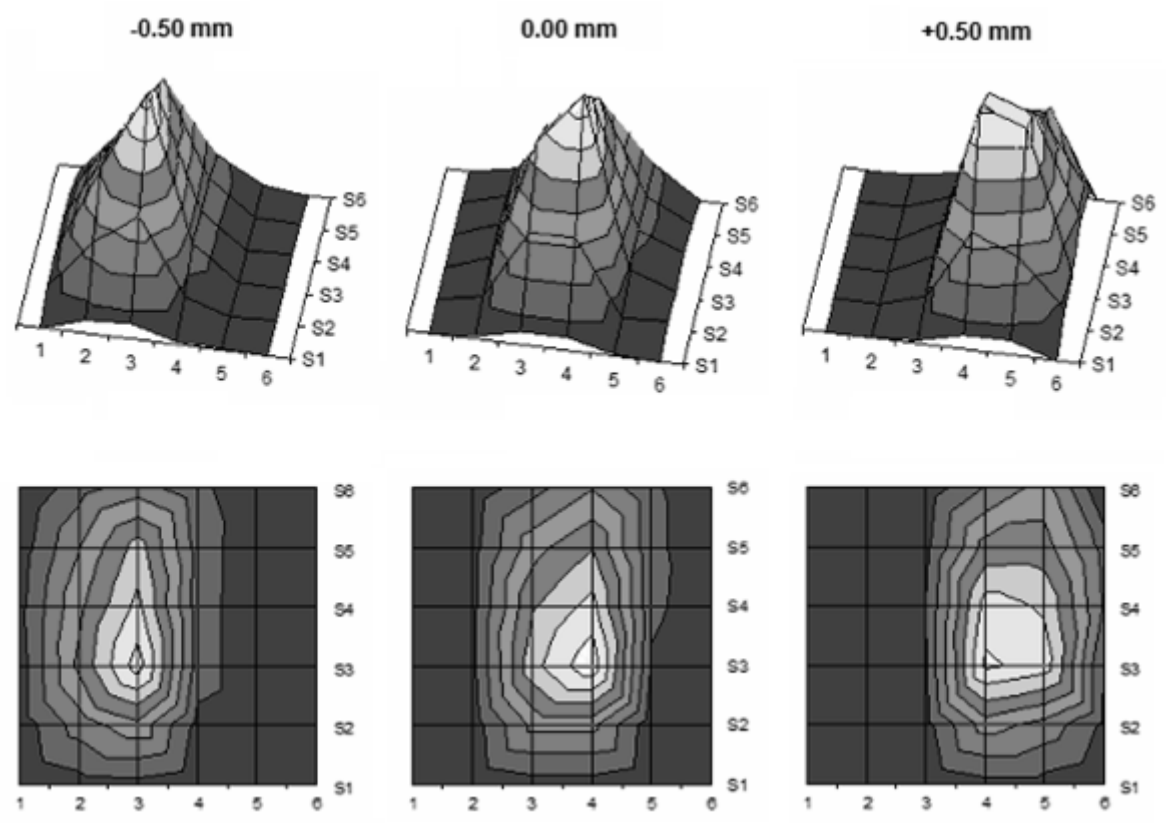

Figure 7. Three different UV Xe-Hg lamp beam two-dimensional profiles. Relative displacements are also indicated.

3.2 Excimer laser beam profiling

UV laser beam profile measurements have been performed under pulsed excitation at λ = 193 nm (Neweks mod. PS100 excimer ArF laser, 4.5 mJ pulse peak energy, 10 ÷ 100 Hz repetition rate): no form of attenuation has been adopted, in order to test the detector performance under high-power UV irradiation. Noise introduced by the laser discharge electronics (embedded thyratron generator) has been avoided by placing the 2D diamond detector 3 m away from the laser output slit. Due to the relatively low-frequency regime of laser repetition rate (100 Hz maximum), digital control circuitry clock frequency has been lowered by synthesizing a new digital prescaler on the main board. Then, a continuous-integration mode was selected and fixed to 10 ms: so, it has been possible to generate the trigger signal for the laser cavity exactly at the maximum repetition rate available (100 Hz).
Two-dimensional profile shown in figure 8 is relative to a single excimer laser pulse: diamond outstanding properties in terms of photoresponse speed and read-out electronics high throughput (up to 2000 samples per second) have allowed to collect, process and display single pulses one by one, even at high repetition rates.

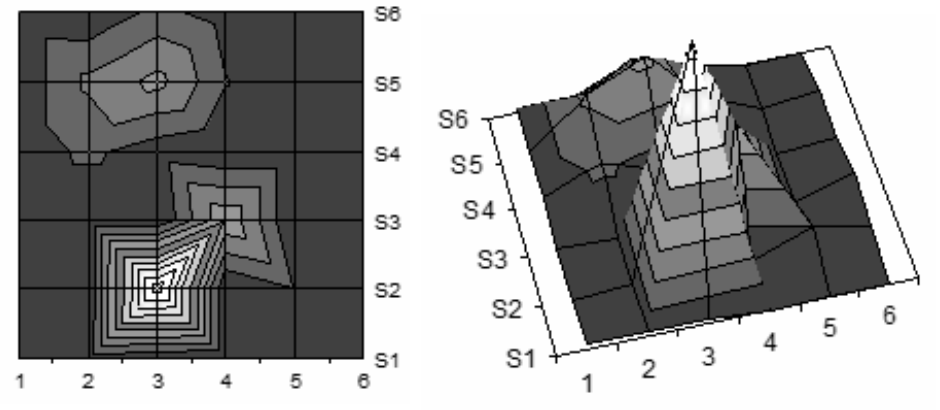

Figure 8. Two-dimensional profile of a single excimer laser pulse (ArF, λ = 193 nm)

Finally, single-pulse profile reported in figure 9 shows a double peak: this laser pulse splitting between a main pulse and a "ghost" pulse is due to an unintentionally introduced cavity misalignment, and is typical of ArF excimer laser sources, as reported elsewhere[12].

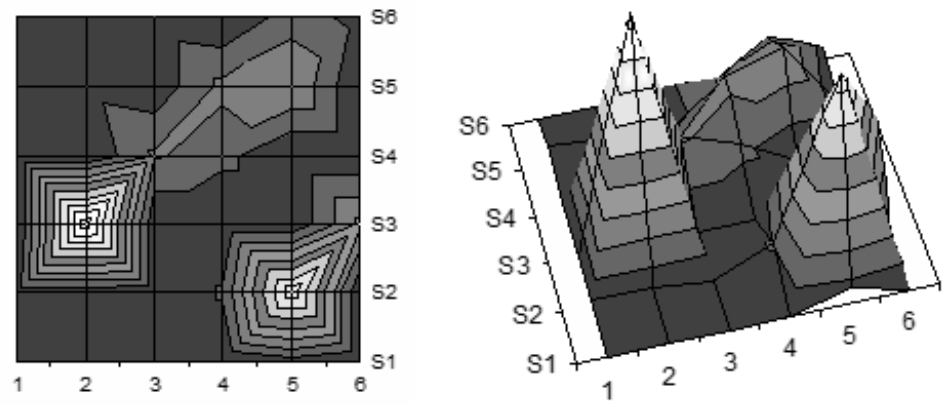

Figure 9. Two-dimensional profile of a single excimer laser pulse in case of cavity misalignment

4. CONCLUSIONS

A complete diamond-based detecting system for 1D and 2D excimer laser beam profiling has been realized and tested. Diamond physical and optical properties, such as radiation hardness and solar blindness, have enabled excimer laser real-time monitoring with no need for attenuators, filters, or wavelength converters. Hence, this work proves that diamond-based UV detecting systems, coupled to fast dedicated multichannel read-out electronics, can definitely compete with commercial UV-enhanced silicon-based devices.

REFERENCES

[1] Gower, M. C., "Industrial applications of laser micromachining," Optics Express 7(2), 56-67 (2000).

[2] Pallikaris, I. G., Siganos, D. G., “Excimer laser in situ keratomileusis and photorefractive keratectomy for correction of high myopia,” Journal of Refractive Corneal Surgery 10, 498-510 (1994).
[3] http://sales.hamamatsu.com/en/products/solid-state-division/si-photodiode-series/si-photodiode/part-s1227-1010bq.php
[4] Whitfield, M., Lansley, S., Gaudin, O., McKeag, R., Rizvi, N., Jackman, R., “Diamond photoconductors: operational lifetime and radiation hardness under deep-UV excimer laser irradiation,” Diamond and Related Materials 10, 715-721 (2001).
[5] Kagan, H., “Recent advantages in diamond detectors development,” Nuclear Instruments and Methods in Physics Research A 541, 221-227 (2005).
[6] Mazzeo, G., Salvatori, S., Rossi, M. C., Conte, G., Castex, M. C., “Deep UV pulsed laser monitoring by CVD diamond sensors,” Sensors and Actuators A 113, 277–281 (2004).
[7] Schein, J., Campbell, K. M., Prasad, R. R., Binder, R., Krishnan, M., “Radiation hard diamond laser beam profiler with subnanosecond temporal resolution,” Review of Scientific Instruments 73(1), 18-22 (2002).
[8] Salvatori, S., Rossi, M. C., Scotti, F., Conte, G., Galluzzi, F., Ralchenko, V., “High-temperature performances of diamond-based UV-photodetectors,” Diamond and Related Materials 9, 982–986 (2000).
[9] Kozlov, S.F., Stuck, R., Hage-Ali, M., Siffert, P., “Preparation and characteristics of natural diamond nuclear radiation detectors,” IEEE Transactions on Nuclear Science 22(1), 160-170 (1975).
[10] Field, J. E., “The Properties of Diamond,” Academic Press, London (1979).
[11] Pernegger, H., Roe, S., Weilhammer, P., “Charge-carrier properties in synthetic single-crystal diamond measured with the transient-current technique,” Journal of Applied Physics 97, 073704 (2005).
[12] Parvin, P., Jaleh, B., Zangeneh, H. R., Zamanipour, Z., Davoud-Abadi, Gh. R., “Excimer laser beam profile recording based on electrochemical etched polycarbonate,” Radiation Measurements 43, 617-622 (2008).